XLIII CILAMCE
21-25, November, 2022
FOZ DO IGUAÇU – PR – BRAZIL

ANALYSIS OF AEROELASTIC STABILITY OF VISCOELASTIC SANDWICH PANELS IN SUBSONIC REGIME USING THE NONPLANAR DOUBLET-LATTICE METHOD

B.S.C. da Cunha[1], A.M.G de Lima[2], D.M. Borges[3]

[1]*Federal University of Uberlândia – School of Mechanical Engineering – Campus Santa Mônica – Uberlândia – MG– Brazil*
brunocarneirocunha@gmail.com
[2]*Federal University of Uberlândia – School of Mechanical Engineering – Campus Santa Mônica – Uberlândia – MG– Brazil*
amglima@mecanica.ufu.br
[3]*Federal University of Uberlândia – School of Mechanical Engineering – Campus Santa Mônica – Uberlândia – MG– Brazil*
dennermiranda@msn.com

Abstract. The engineers of aeronautical industries are frequently facing with subsonic panel flutter phenomena, where the design and analyses of aerospace vehicles requires the knowledge of their critical flutter speeds for safety requirements and to avoid catastrophes. Thus, whenever possible it is important to evaluate efficient and low-cost aeroelastic control strategies to deal with the problem of panel flutter phenomenon. In this context, the use of passive constraining viscoelastic layers seems to be an interesting alternative to be used in such situations. However, the structural and aerodynamic modeling procedures of an aeroviscoelastic system subjected to a subsonic airflow are not easy. In most of the cases, the difficult is related to the fact that, the viscoelastic behavior depends strongly on the excitation frequency and temperature, resulting in some difficulties during the coupling between the structural and aerodynamic models to account for the unsteady aerodynamics and complex behavior of the viscoelastic part, simultaneously. In this study, it is proposed an efficient numerical strategy to model aeroviscoelastic systems under subsonic airflows for panel flutter suppression. Here, the curved plate model of a thin three-layer sandwich panel and aerodynamic loadings using the nonplanar doublet lattice method are constructed both in MATLAB® environment code. Also, to solve the resulting equations of motion of the complex aeroviscoelastic system, an improved version of the p-k method is proposed herein to estimate the critical flutter speeds and to verify the possibility of increasing the critical flutter speeds of the base panel by using viscoelastic materials. The influence of design parameters characterizing the performance of the viscoelastic treatment and its operation temperature on the flutter boundary has been also addressed herein.

Keywords: Flutter suppression, viscoelastic materials, unsteady aerodynamic, doublet lattice method Introduction

1.Introduction

The problem of panel flutter suppression has been studied by many authors in the open literature [10,13,15,18-20,27-28] to improve the aeroelastic efficiency of the resulting systems and to avoid catastrophes. As an example, Stanford et al. [36] and Alyanak and Pendleton [2] have studied the influence of the composite fiber orientations, tow steering and variable fiber spacing on the critical flutter speeds of composite plates. In this line, the viscoelastic materials have been also commonly used in aeronautical and aerospace industries due to their low cost of application and maintenance and their efficiency in mitigating undesired vibrations [4-5,7,12-14,25-26]. Thus, it is expected that, the use of constrained viscoelastic layers (CVLs) is also an efficient aeroelastic control technique to deal with the problem of panel flutter, as shown

in [13] for the case of supersonic panel flutter boundary. However, few works have dedicated to the use of passive CVLs to the case of aeroelastic systems under subsonic airflows, which motivates the present contribution.

In the open literature, most of the applications involving the use of viscoelastic materials in flutter suppression are related to supersonic panel flutter conditions, generally using methodologies such as the Piston theory to model the aerodynamic loadings acting on the panels [13]. Merret [27] has performed an analytical investigation of the degree of influence of a viscoelastic treatment on the flutter velocity of a plate system in time and frequency domains. Cunha-Filho et al. [13] have studied the possibility of applying passive CVLs to increase the critical flutter speeds of a flat panel subjected to a supersonic flow by conveniently accounting for the frequency and temperature dependent behavior of the viscoelastic material.

In terms of practical applications, the use of viscoelastic materials has some advantages among others passive control methods such as inherent stability, effectively in broad frequency band and low cost of application and maintenance [12,25-26]. Despite these advantages, the sensitivity of these materials under operational and environmental variations must be not disregarded and it must be conveniently accounted for in the modeling to guarantee their maximum of efficiency and to establish their limitations to a desired aeroelastic application. However, most of aerodynamic modeling of aeroelastic systems incorporating viscoelastic materials for flutter suppression has been performed using linearized and/or simplified techniques. Among these applications, the Piston theory has been widely used in applications involved supersonic airflow regimes [13,24]. Another commonly used technique to deal with this kind of aeroviscoelastic problem is the so-called Strip theory [37], which gives the increment aerodynamic loading necessary to estimate the critical flutter speeds of an aeroviscoelastic system. However, the estimation of the critical flutter boundary of an aeroviscoelastic problem under subsonic airflows by using an unsteady aerodynamic modeling methodology such as the nonplanar Doublet-Lattice method (DLM) [1,8-9,11,17,21-23,29-35,38-42] is not numerous in the literature, which motivates the present study. In parts, it is due to the inherent difficult in dealing with the complex behavior of the viscoelastic substructure in the unsteady aerodynamics. In addition, modifications on the p-k method must be performed in order to account for the complex behavior of the aeroviscoelastic system under subsonic regime to estimate its critical flutter speeds with accuracy.

Thus, in the present study, an efficient numerical strategy is proposed to model aeroviscoelastic systems subjected to subsonic airflows for the flutter suppression. Within this aim, the finite element (FE) method is used to model the viscoelastic sandwich curved panel of interest and the nonplanar DLM is used to generate the unsteady aerodynamic loadings acting on it. The DLM take advantages over another aerodynamics modeling methodology due to its ability to extend over multiple lift surfaces with reliability and low computational cost compared with the high-fidelity computational fluid dynamics (CFD) methods, for instance. It explains the fact that, it is still extensively used today in aeronautical and aerospace industries to perform unsteady aerodynamic loadings, even for more complex aircraft configurations.

Therefore, it is used the nonplanar DLM available in the MATLAB® environment code to generate the unsteady aerodynamic loadings acting on the sandwich curved panel with CVL modeled by using the MATLAB® program. The interest is to solve the equations of motion of the resulting aeroviscoelastic system under subsonic conditions using an improved modified version of the p-k method [19] to deal with this kind of problem. Again, it is important to highlight that, despite the nonplanar DLM is a common method used in industry to solve aeroelastic problems, few works have proposed its use to model aeroelastic systems with passive CVLs subjected to subsonic airflow for flutter suppression. Then, apart from the practical numerical tool which is proposed herein, it is demonstrated the possibility of increasing the critical flutter speeds of aeronautical panels under subsonic airflows.

2.Background on the DLM modeling methodology

According to Van Zyl [38-42], the Doublet-Lattice Method (DLM) is a finite element method for the solution of the oscillatory subsonic pressure-downwash integral equation for multiple surfaces. It is one of the most applied methods to study non-stationary aerodynamic loadings that considers the fluid compressible. The DLM is a potential flow proposed originally by Albano [1] to solve unsteady aerodynamic flows across a surface. Based on the work by Kotikalpudi [22], the DLM give a frequency response for a pressure distribution on an oscillating structure in steady flows, for a specific frequency. Therefore, it is a useful tool in preliminary phases and use world-wide for aeronautical project in combination with the FE method to estimate the critical flutter boundary and dynamic response analyses at subsonic speeds.

In nonplanar DLM method, the dimensionless normalwash is given as [34]:

$$w(x,s) = \left(\pi/8\right) \sum_{n=1}^{N} \iint K(x,\xi,s,\sigma) p(\xi,\sigma) d\xi d\sigma \tag{1}$$

where $p(\xi,\sigma)$ is the complex amplitude of lifting pressure coefficient, (x,s) are the orthogonal coordinates on the n-th surface *S*, *K* is the complex acceleration potential kernel for oscillatory subsonic flow. This later can be solved by using a parabolic [30] or quartic [33] approximations. Thus, the recent refinement is based on an improvement of the Kernel function that has been given in the preliminary form, according to [34]:

$$K = \left(\frac{K_1 T_1}{r^2} + \frac{K_2 T_2}{r^4} \right) exp\left(- \frac{i\omega x_0}{U_\infty} \right) \tag{2}$$

In Eq. (2), ω is the frequency, x_0 is the distance between the sending and receiving points parallel to the freestream and U is the velocity of the freestream. $T_1 = \cos\left(\gamma_r - \gamma_s\right)$, $T_2 = \left(z_0 \cos\gamma_r - y_0 sen\gamma_r\right)\left(z_0 \cos\gamma_s - y_0 sen\gamma_s\right)$, with, $r^2 = z^2_0 + y^2_0$, y_0 and z_0 are, respectively, the cartesian distances between the sending and receiving points perpendicular to the freestream and γ_r and γ_s are the dihedral angles of the receiving and sending points, respectively, as illustrated in Fig. 1.The planar and nonplanar contributions of the Kernel are given by the relations:

$$K_1 = I_1 + \left[\frac{Mr}{R} \right] \left[\frac{exp\left(-iku_1\right)}{\left(1+u^2_1\right)^{1/2}} \right] \tag{3.a}$$

$$K_2 = -3I_2 - \left[\frac{ikM^2r^2}{R^2} \right] \left[\frac{exp\left(-iku_1\right)}{\left(1+u^2_1\right)^{1/2}} \right] - \frac{Mr}{R} \left[\left(1+u^2_1\right) \left(\frac{\beta^2 r^2}{R^2} \right) + 2 + \left(\frac{Mru_1}{R} \right) \right] \tag{3.b}$$

where: M is Mach number, $\beta = \left(1-M^2\right)^{1/2}$, $u_1 = \dfrac{\left(MR - x_0\right)}{\beta^2 r}$, $R = \left(x^2_0 + \beta^2 r^2\right)^{1/2}$ and $k = \dfrac{\omega r}{U_\infty}$.

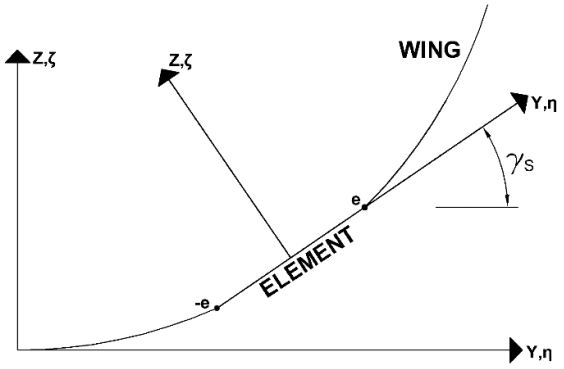

Figure 1. Lifting surface coordinate system.

According to Rodden et. al. [30], the integration of I_1 and I_2 by parts once gives as:

$$I_1(u_1,k) = exp(-iku_1)\left[1 - \frac{u_1}{(1+u^2_1)^{1/2}} - ikI_0(u_1,k)\right] \tag{4.a}$$

$$I_2(u_1,k) = \frac{exp(-iku_1)}{3}\left\{(2+iku_1)\left(1 - \frac{u_1}{(1+u^2_1)^{1/2}}\right)\ldots - \frac{u_1}{(1+u^2_1)^{3/2}} - ikI_0(u_1,k) + k^2J_0(u_1,k)\right\} \tag{4.b}$$

The integrals I_0 and J_0 can be evaluated using approximation to $u(1+u^2)^{-1/2}$ proposed by Laschka [23] for $u \geq 0$, such as:

$$I_0(u_1,k) \cong \sum_{n=1}^{11} \frac{a_n exp(-ncu_1)}{n^2c^2+k^2}(nc-ik) \tag{5.a}$$

$$J_0(u_1,k) \cong \sum_{n=1}^{11} \frac{a_n exp(-ncu_1)}{(n^2c^2+k^2)^2}\left\{(n^2c^2-k^2) + ncu_1(n^2c^2+k^2)\ldots - ik\left[2nc + u_1(n^2c^2+k^2)\right]\right\} \tag{5.b}$$

Otherwise, for $u < 0$, it has been taken advantage of symmetry, in this case:

$$I_1(u_1,k) = 2Re\left[I_1(0,k)\right] - Re\left[I_1(-u_1,k)\right] + i\ Im\left[I_1(-u_1,k)\right] \tag{6.a}$$

$$I_2(u_1,k) = 2Re\left[I_2(0,k)\right] - Re\left[I_2(-u_1,k)\right] + i\ Im\left[I_2(-u_1,k)\right] \tag{6.b}$$

where, $c = 0.372$ and the coefficients are given in Tab. 1.

Table 1 – Coefficients in Laschka's approximation to $u(1+u^2)^{-1/2}$.

n	a_n
1	0,24186198

2	-2,7918027
3	24,991079
4	-111,59196
5	271,43549
6	-305,75288
7	-41,183630
8	545,98537
9	-644,78155
10	328,72755
11	-64,279511

At zero frequency the planar and nonplanar part of the kernel is given as:

$$K_{10} = \lim_{\omega \to 0} K_1 = 1 + \frac{x_0}{R} \tag{7.a}$$

$$K_{20} = \lim_{\omega \to 0} K_2 = -2 - \left(\frac{x_0}{R}\right)\left(2 + \frac{\beta^2 r^2}{R^2}\right) \tag{7.b}$$

The original method assumed that the lifting pressure could be concentrated along a line, it is located at the 1/4 chord line of the element and the surface boundary condition is a prescribed normalwash at the control point of each box which is located at the 3/4 chord point along the centerline of each box.

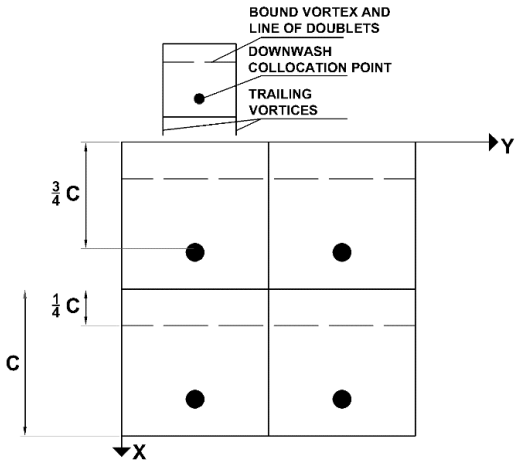

Figure 2. Lifting surface coordinate system.

The numerical form of the integral in Eq. (1), becomes:

$$\{w\} = \left[D_{rs}\right]\{p\} \tag{8}$$

$$D_{rs} = \left(\frac{\Delta x_s}{8\pi}\right)\int_{-e}^{+e}\left(\frac{K_1 T_1}{r^2} + \frac{K_2 T_2}{r^4}\right) exp\left[\frac{-i\,\omega\left(x_0 - \bar{\eta}\tan\lambda_s\right)}{U_\infty}\right] d\bar{\eta} \tag{9}$$

So, the evaluation of the normalwash factor Eq. (8) by adding and subtracting the steady values of $K_1$and K_2, denoted by K_{10} and K_{20} . Then, Eq. (9) gives as [34]:

$$D_{rs} = D_{0rs} + D_{1rs} + D_{2rs} \tag{10}$$

where D_{0rs}, D_{1rs} and D_{2rs} are the components, respectively, steady, planar and nonplanar unsteady, represented by, $D_{0rs} = \left(\frac{\Delta x_s}{8\pi}\right)\int_{-e}^{+e}\left(\frac{K_{10}T_1}{r^2} + \frac{K_{20}T_2}{r^4}\right)\mathrm{d}\bar{\eta}$, $D_{1rs} = \left(\frac{\Delta x_s}{8\pi}\right)\int_{-e}^{+e}\frac{Q_1(\bar{\eta})}{r^2}\mathrm{d}\bar{\eta}$ and $D_{2rs} = \left(\frac{\Delta x_s}{8\pi}\right)\int_{-e}^{+e}\frac{Q_2(\bar{\eta})}{r^4}\mathrm{d}\bar{\eta}$.

Its necessary estimate the incremental oscillatory normalwash factor by an interpolation of the numerators as quartics form, such as:

$$Q_1(\bar{\eta}) = A_1\bar{\eta}^2 + B_1\bar{\eta} + C_1 + D_1\bar{\eta}^3 + E_1\bar{\eta}^4 \cong \left\{K_1 exp\left[-i\omega\left(x_0 - \bar{\eta}\tan\lambda_s\right)/U_\infty\right] - K_{10}\right\}T_1 \tag{11.a}$$

$$Q_2(\bar{\eta}) = A_2\bar{\eta}^2 + B_2\bar{\eta} + C_2 + D_2\bar{\eta}^3 + E_2\bar{\eta}^4 \cong \left\{K_2 exp\left[-i\omega\left(x_0 - \bar{\eta}\tan\lambda_s\right)/U_\infty\right] - K_{20}\right\}T_2 \tag{11.b}$$

It is indispensable to emphasize that the inboard, inboard intermediate, center, outboard intermediate and outboard values of $Q_1(\bar{\eta})$ along a line of the lifting pressure, respectively by $Q_1(-e)$, $Q_1(-e/2)$, $Q_1(0)$, $Q_1(e/2)$ and $Q_1(e)$. So, the coefficients are:

$$A_1 = -\frac{1}{6e^2}\left[Q_1(-e) - 16Q_1\left(-e/2\right) + 30Q_1(0) - 16Q_1\left(e/2\right) + Q_1(e)\right] \tag{12.a}$$

$$B_1 = \frac{1}{6e^2}\left[Q_1(-e) - 8Q_1\left(-e/2\right) + 8Q_1\left(e/2\right) - Q_1(e)\right] \tag{12.b}$$

$$C_1 = Q_1(0) \tag{12.c}$$

$$D_1 = -\frac{2}{3e^3}\left[Q_1(-e) - 2Q_1\left(-e/2\right) + 2Q_1\left(e/2\right) - Q_1(e)\right] \tag{12.d}$$

$$E_1 = \frac{2}{3e^4}\left[Q_1(-e) - 4Q_1\left(-e/2\right) + 6Q_1(0) - 4Q_1\left(e/2\right) + Q_1(e)\right] \tag{12.e}$$

The same previous proceedings are taken account to $Q_2(\bar{\eta})$. Then, the planar downwash factor becomes:

$$\begin{aligned} D_{1rs} = \frac{\Delta x_s}{8\pi}\Big\{&\left[(\bar{y}^2 - \bar{z}^2)A_1 + \bar{y}B_1 + C_1 + \bar{y}(\bar{y}^2 - 3\bar{z}^2)D_1 + (\bar{y}^4 - 6\bar{y}^2\bar{z}^2 + \bar{z}^4)E_1\right]F \ldots \\ &+\left[\bar{y}A_1 + \frac{1}{2}B_1 + \frac{1}{2}(3\bar{y}^2 - \bar{z}^2)D_1 + 2\bar{y}(\bar{y}^2 - \bar{z}^2)E_1\right]\log\frac{(\bar{y}-e)^2 + \bar{z}^2}{(\bar{y}+e)^2 + \bar{z}^2} + \ldots \\ &+2e\left[A_1 + 2\bar{y}D_1 + \left(3\bar{y}^2 - \bar{z}^2 + \frac{1}{3}e^2\right)E_1\right]\Big\} \end{aligned} \tag{13}$$

where: $F = \delta_1\frac{2e}{\bar{y}^2 + \bar{z}^2 - e^2}\left(1 - \varepsilon\frac{\bar{z}^2}{e^2}\right) + \delta_2\frac{\pi}{|\bar{z}|}$, $\varepsilon = \frac{e^2}{\bar{z}^2}\left[1 - \frac{\bar{y}^2 + \bar{z}^2 - e^2}{2e|\bar{z}|}a\tan\left(\frac{2e|\bar{z}|}{\bar{y}^2 + \bar{z}^2 - e^2}\right)\right]$

Then, the nonplanar downwash factor is, when $|(\bar{y}^2 + \bar{z}^2 - e^2)/2e\bar{z}| \leq 0.1$, given as:

$$D_{2rs} = \frac{\Delta x_s}{16\pi\bar{z}^2}\left\{\left[(\bar{y}^2 + \bar{z}^2)A_2 + \bar{y}B_2 + C_2 + \bar{y}(\bar{y}^2 + 3\bar{z}^2)D_2 + (\bar{y}^4 + 6\bar{y}^2\bar{z}^2 - \bar{z}^4)E_2\right]F \ldots\right.$$

$$+\frac{1}{(\bar{y}+e)^2+\bar{z}^2}\left\{\left[\left(\bar{y}^2+\bar{z}^2\right)\bar{y}+\left(\bar{y}^2+\bar{z}^2\right)e\right]A_2+\left(\bar{y}^2+\bar{z}^2+\bar{y}e\right)B_2+(\bar{y}+e)C_2\ldots\right.$$
$$\left.+\left[\bar{y}^4-\bar{z}^4+\left(\bar{y}^2-3\bar{z}^2\right)\bar{y}e\right]D_2+\left[\left(\bar{y}^4-2\bar{y}^2\bar{z}^2-3\bar{z}^4\right)\bar{y}+\left(\bar{y}^4-6\bar{y}^2\bar{z}^2+\bar{z}^4\right)e\right]E_2\right\}\ldots$$
$$-\frac{1}{(\bar{y}-e)^2+\bar{z}^2}\left\{\left[\left(\bar{y}^2+\bar{z}^2\right)\bar{y}-\left(\bar{y}^2-\bar{z}^2\right)e\right]A_2+\left(\bar{y}^2+\bar{z}^2-\bar{y}e\right)B_2+(\bar{y}-e)C_2\ldots\right.$$
$$\left.+\left[\bar{y}^4-\bar{z}^4-\left(\bar{y}^2-3\bar{z}^2\right)\bar{y}e\right]D_2+\left[\left(\bar{y}^4-2\bar{y}^2\bar{z}^2-3\bar{z}^4\right)\bar{y}-\left(\bar{y}^4-6\bar{y}^2\bar{z}^2+\bar{z}^4\right)e\right]E_2\right\}$$
$$\left.+\left[\bar{z}^2\log\frac{(\bar{y}-e)^2+\bar{z}^2}{(\bar{y}+e)^2+\bar{z}^2}\right]D_2+4\bar{z}^2\left[e+\bar{y}\log\frac{(\bar{y}-e)^2+\bar{z}^2}{(\bar{y}+e)^2+\bar{z}^2}\right]E_2\right\} \tag{14}$$

To the general cases:

$$D_{2rs}=\frac{e\Delta x_s}{8\pi\left(\bar{y}^2+\bar{z}^2-e^2\right)}\left\{\frac{1}{\left[(\bar{y}+e)^2+\bar{z}^2\right]\left[(\bar{y}-e)^2+\bar{z}^2\right]}\ldots\right.$$
$$\times\left\{2\left(\bar{y}^2+\bar{z}^2+e^2\right)\left(e^2A_2+C_2\right)+4\bar{y}e^2B_2+2\bar{y}\left(\bar{y}^4-2e^2\bar{y}^2+2\bar{y}^2\bar{z}^2+3e^4+2e^2\bar{z}^2+\bar{y}^4\right)D_2\ldots\right.$$
$$\left.+\ 2\left(3\bar{y}^6-7e^2\bar{y}^4+5\bar{y}^4\bar{z}^2+6e^4\bar{y}^2+6e^2\bar{y}^2\bar{z}^2-3e^2\bar{z}^4-\bar{z}^6+\bar{y}^2\bar{z}^4-2e^4\bar{z}^2\right)E_2\right\}\ldots$$
$$-\frac{\left(\delta_1\varepsilon+\Delta\right)}{e^2}\left[\left(\bar{y}^2+\bar{z}^2\right)A_2+\bar{y}B_2+C_2+\bar{y}\left(\bar{y}^2+3\bar{z}^2\right)D_2+\left(\bar{y}^4+6\bar{y}^2\bar{z}^2-3\bar{z}^4\right)E_2\right]\Big\}\ldots$$
$$\left.+\frac{\Delta x_s}{8\pi}\left\{\left[\frac{D_2}{2}\log\frac{(\bar{y}-e)^2+\bar{z}^2}{(\bar{y}+e)^2+\bar{z}^2}\right]+2\left[e+\bar{y}\log\frac{(\bar{y}-e)^2+\bar{z}^2}{(\bar{y}+e)^2+\bar{z}^2}\right]E_2\right\}\right. \tag{15}$$

where: $\Delta=\left(\frac{e}{|\bar{z}|}\right)^2\left\{1-\delta_1-\delta_2\frac{\pi}{|\bar{z}|}\left(\frac{\bar{y}^2+\bar{z}^2-e^2}{2e}\right)\right\}$, $\delta_1=1,\delta_2=0$ to $\bar{y}^2+\bar{z}^2-e^2>0$, $\delta_1=1,\delta_2=\frac{1}{2}$ to $\bar{y}^2+\bar{z}^2-e^2=0$

and $\delta_1=1,\delta_2=1$ to $\bar{y}^2+\bar{z}^2-e^2<0$.

Finally, the matrix $AIC=[D]^{-1}$ represents the influence aerodynamic of the unsteady flow around the structure.

3.Viscoelastic modeling

The use of viscoelastic materials has been regarded as a convenient strategy in many types of industrial applications, that these materials can be applied either as discrete device or surface treatments [12-13, 25-26]. Another interesting strategy consists in incorporating viscoelastic materials as a means of adding damping to vibration neutralizes by Lima et al [24-25]. As a result, it is currently possible to perform finite element modeling of complex real-world engineering structures such as automobiles, airplanes, communication satellites, buildings, and space structures.

According to the linear theory of viscoelastic the one-dimensional stress-strain relation can be expressed, in Laplace domain, as follows:

$$\sigma(s)=\left(G_r+H(s)\right)\varepsilon(s) \tag{16}$$

In the Eq. 16, G_r is the static modulus, representing the elastic behavior and $H(s)$ is the relaxation function, associated to the dissipation effects. When evaluated the imaginary axis of the s-plane $s=(i\omega)$, the Eq. 16 can be expressed under the following form [24]:

$$G(\omega)=G'(\omega)+iG''(\omega)=G'(\omega)(1+i\eta(\omega)) \tag{17}$$

where $G'(\omega)$, $G''(\omega)$ and $\eta(\omega) = G''(\omega)/G'(\omega)$ are the storage and loss moduli and loss factor, respectively. The complex modulus provides a straightforward model the viscoelastic behavior in the frequency domain.

The complex modulus function, that represents the reduce frequency and temperature of the viscoelastic material 3M™ ISD112, can be written as [24-25]:

$$G(\omega,T_v) = 0.4307 + \frac{1200}{1 + 3.24\left(\frac{i\omega_r}{1543000}\right)^{-0.18} + \left(\frac{i\omega_r}{1543000}\right)^{-0.6847}} [MPa] \tag{18}$$

where: $\alpha(T_V) = 10^{\left(-3758.4\left(\frac{1}{T_v} - 0.00345\right) - 225.06\log\left(0.00345T_v\right) + 0.23273\left(T_v - 290\right)\right)}$ is the displacement factor and $\omega_r = \alpha\left(T_v\right)$ is the reduce frequency.

The properties of viscoelastic system depend on of environment conditions. So, the temperature and frequency are usually considered to be both the most important environmental factors which exerts influence upon the properties of viscoelastic materials. Then, it becomes important to taking into account for variations in the modeling of viscoelastic stiffness. This can be done by making use of the called Frequency Temperature Superposition Principle – FTSP, which establishes a relation between the effects of the excitation frequency and temperature on the properties of the thermorheologically viscoelastic materials [24].

4.Discretization based on finite element

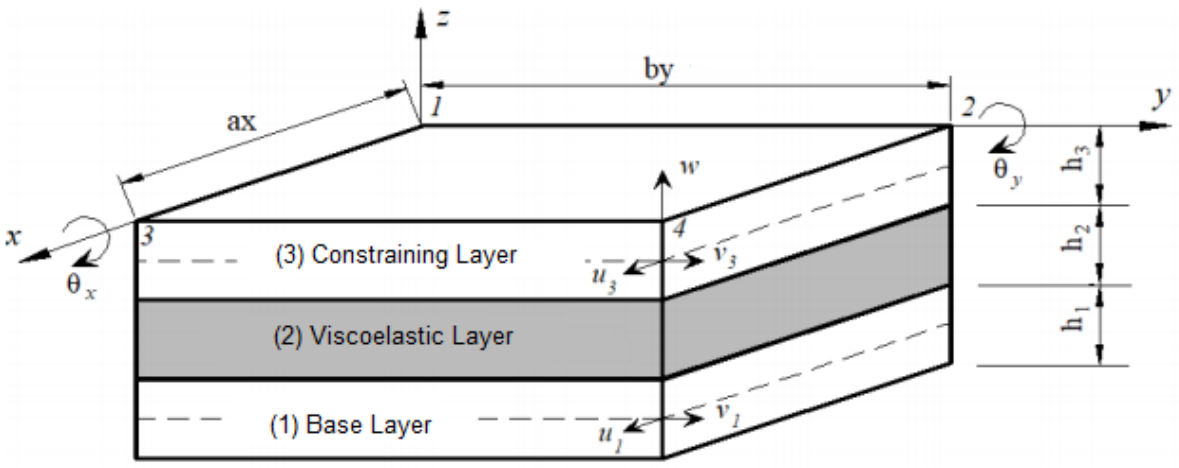

Figure 3. Illustration of a sandwich plate with three layer [24].

For this article, has been applied a curve rectangular plate with four nodes and seven degrees-of-freedom (DOFs) per each elementary node in the Fig. 3, according to developments by Lima et al. [26]. Thus, the sandwich modeling is composed by: (a) elastic base-plate, (b) viscoelastic core and (c) elastic constraining layer. So, the DOFs are: displacements in the middle plane of base-plate in directions x and y (denoted by u_1 and v_1, respectively); displacements in the middle plane of constraining layer u_3 and v_3; transverse displacements w; the cross-section rotations $\theta_x = \partial w/\partial x$ and $\theta_y = \partial w/\partial y$. The terms a and b , represent, respectively, the dimensions of the element in the direction x and y .

Formerly, the following assumptions are adopted: (i) all materials are homogeneous, isotropic and linear behavior; (ii) normal strains in direction z are null; (iii) the elastic layers are modeled by Kirchhoff's theory; (iv) the viscoelastic layer adopted Mindlin's theory; (v) the cross-section rotation θ_x and θ_y are equal to elastic layers; (vi) the transverse displacement is the same for all the layers. Then, the discretization of the displacement fields and transverse is, respectively, by linear and cubic function, according to the relation, $U(x,y) = N(x,y)\delta_{(e)}(t)$, that $N(x,y)$ is the matrix formed by the shape functions, $\delta_j = \left[u_{1j} \; v_{1j} \; u_{3j} \; v_{3j} \; w_j \; \theta_{xj} \; u_{yj} \right]^T$ with $j = 1-4$ represents the vector of vector of nodal variables. The strains-displacement is, $\varepsilon(x,y) = D(x,y)\delta$, and the strains of elastic layers, $\varepsilon_i = \left[\varepsilon_x^i \; \varepsilon_y^i \; \gamma_{xy}^i \right]^T$ with $i = 1,3$, and for the viscoelastic core, $\varepsilon_2 = \left[\varepsilon_x^2 \; \varepsilon_y^2 \; \gamma_{xy}^2 \; \gamma_{xz}^2 \; \gamma_{yz}^2 \right]^T$. So, the stress can be give as:

$$S(x,y,t) = C\varepsilon(x,y,t) = CD(x,y)\delta_{(e)}(t) \tag{19}$$

where C_i $(i = 1,3)$ is the isotropic elastic material properties matrix, $C_2(\omega,T)$ contains the frequency-temperature-dependent material properties and $D(x,y)$ is formed for each layer by strain-displacement relations [25].

The strain and kinetic energies of three-layer sandwich plate FE are formulated and the elementary mass and stiffness matrices can be obtained as:

$$M^{(e)} = \sum_{i=1}^{3} \rho_i h_i \int_{x=0}^{a} \int_{y=0}^{b} N^T(x,y) N(x,y) dy dx \tag{20.a}$$

$$K_e^{(e)} = \sum_{i=1,3} \int_{z=0}^{h_i} \int_{x=0}^{a} \int_{y=0}^{b} D_i^T(x,y) C_i D_i(x,y) dy dx dz \tag{20.b}$$

$$K_2^{(e)}(\omega,T) = \int_{z=0}^{h_2} \int_{x=0}^{a} \int_{y=0}^{b} D_2^T(x,y) C_2(\omega,T) D_2(x,y) dy dx dz \tag{20.c}$$

where h_i and ρ_i is the thickness and the mass density of the i-th layer, respectively. Thus, can be noted the contribution of purely elastic and viscoelastic parts in the sandwich structure, by the matrix $K_e^{(e)} = K_1^{(e)} + K_2^{(e)}$ and $K_2^{(e)}$, respectively.

In that way, the elementary equations of motion are such as:

$$M^{(e)} \ddot{u}_{(e)}(t) + \left[K_e^{(e)} + K_v^{(e)} \right] u_{(e)}(t) = f^{(e)}(t) \tag{21}$$

where $M^{(e)}$, $K_e^{(e)}$, $K_v^{(e)}$, $u^{(e)}$ and $f^{(e)}$ are the mass matrix, the elastic stiffness matrix, the viscoelastic matrix, the vectors of generalized displacements and external loads, respectively.

5.Aerodynamics modeling

The aerodynamic model must be capable of interacting effectively with the structure to be able to calculate the aeroviscoelastic behavior of the system and, consequently, calculate the flutter velocity. So, it is necessary to generate the normalwash through the aerodynamic force distribution for a single deformation that is given for the structural mesh. In addition, the effect of aerodynamic forces applied in the structural model should be computed to the system. Finally, has been desired the model in the frequency domain to analyze the aeroviscoelastic interactions [22].

Then, it is taken the medium plane of the structure and approximate by generic polynomial interpolation. So, it is necessary to evaluate the equation of motion and the method of FE to acquire the displacements of each node and give as:

$$\left\{F_{modal}\right\}=\left[M_S\right]\{\ddot{\eta}\}+\left[K_S\eta\right] \tag{22}$$

where F_{modal}, S and η are the external loads, subindex of structure and nodes displacements, respectively.

So, the elastic deformation of i-th node in the structure can be given by δ_i and in function of the modal coordinates using the j-th mode of vibration θ_i such as, $\delta_i=\sum_{j}^{M}\phi_{ij}\eta_j$.In that way, the loads acting in the control point of the panel is relating of the aerodynamics influence coefficients (AIC) that has been obtained by non-planar method doublet-lattice [22].

$$\left\{F_{aero}\right\}=q_\infty\left\{T_{as}\right\}^T[S]\left\{w_N\right\}[AIC]\left\{T_{as}\right\}\left\{\theta_i\right\} \tag{23}$$

where $T_{as}=\left[T_{interp}\right]\left[T_{spline}\right]$ represents the polynomial function $\left[T_{interp}\right]=\sum_{j=0}^{nx}\sum_{k=0}^{ny}\alpha_{jk}X_\alpha^jY_\alpha^k$ and the $\left[T_{spline}\right]$ the medium plane located at ¾ of the chord line in the aerodynamic mesh. So, the constants of approximate of modal forms $\left(\alpha_{jk}=\left[T_{spline}\right]h_{modal}\right)$ is calculate by the interpolation of displacements (h_{modal}) in each node has been acquired by the mesh structured at ¾ of chord line. The variables X and Y are the coordinates of the nodes. Therefore, the downwash, $\left\{w_N\right\}=\frac{\partial h_a}{\partial t}+U\frac{\partial h_a}{\partial x}$ is resolved by the displacements of nodes, in other words, $h_a=T_{as}$ [22].

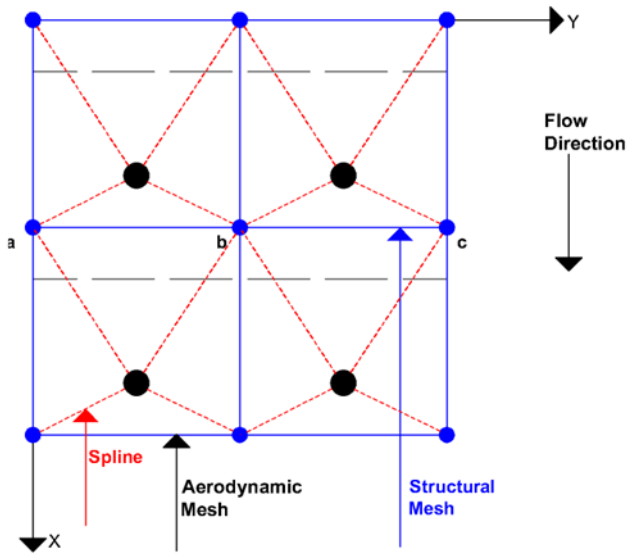

Figure 4. Example of the interaction between the structural and aerodynamic mesh.

In that way, to connect the structure and aerodynamic modeling it is necessary to chance de matrix T_{as}, gives as, $\{F_{modal}\}=\{\phi\}^T\left[T_{as}\right]^T\{F_{aero}\}$. Then, the distribution of aerodynamic loads along the structure is $\{F_{modal}\}=q_\infty\left[Q_j\right]\eta$. Thus, combining all these equations leads to generalized aerodynamic matrix (GAM), represents by [22]:

$$\left[Q_j\right]=\left\{\theta_j\right\}^T\left\{T_{as}\right\}^T[S]\left\{w_N\right\}[AIC]\left\{T_{as}\right\}\left\{h_{modal}\right\}\left\{\theta_j\right\} \tag{24}$$

where $q_\infty = (1/2)\rho_{ar}U_\infty^2$ and the matrix GAM is dependent of the Mack number and the reduced frequency.

Therefore, it is necessary to evaluate the stability of the system analyze the eigenvalues of it. Then, when the imaginary part of this becomes positive, is an unstable system. However, the GAM is a complex matrix, that makes the analysis of stability more complicated, because the reduced frequency of the system depending on the natural frequencies. This means that the problem of the eigenvalues to be solved is nonlinear. Finally, some methods have been developed to solve the problem of nonlinear eigenvalues associated with aeroelastic or aeroviscoelastic stability like PK method [22].

6.PK-Method of flutter solution

The equation for modal flutter analysis using the PK-method as Rodden and Johnson [33]:

$$\left(p^2M + K - \frac{\varrho_{ar}U_\infty^2}{2}Q(k)\right)\{\eta\} = 0 \tag{25}$$

where b, $k = \omega b/U_\infty$ and p are the characteristic length, reduced frequency and eigenvalue, respectively.

For the solution of PK-method, the Eq. 20 is rewritten in the state-space form, $[A - pI]\{\eta\}$, as:

$$[A] = \begin{bmatrix} 0 & I \\ -M^{-1}\left(K - \frac{\varrho_{ar}U_\infty^2 Re(Q)}{2}\right) & -M^{-1}\left(-\frac{\varrho_{ar}bU_\infty Im(Q)}{4k}\right) \end{bmatrix} \tag{26}$$

Thus, the iteration for the complex roots, the complex pairs of eigenvalues has been found as $p = \omega\left(\frac{g}{2} \pm i\right)$, where $\omega = Im(p)$ and $g = \frac{2Re(g)}{Im(p)}$. So, the stopping criteria to reduced frequency as, $\left|k_s^{(j)} - k_s^{(j-1)}\right| < \varepsilon \rightarrow k_s^{(j-1)} < 1$ and $\left|k_s^{(j)} - k_s^{(j-1)}\right| < \varepsilon k_s^{(j-1)} \rightarrow k_s^{(j-1)} \geq 1$. Where the term j represents the j-th step of the loop, s is the reduced frequency for the actual mode of vibration and ε is the tolerance which for rule is 0.001 [33].

7.Results and discussion

7.1.Curved plate without viscoelastic material

Initially, it is necessary to verify the curved plate without the viscoelastic material. Then, in the Fig. 5 the proposed model is shown for the initial simulations. So, the Tab. 2 and 3 are, respectively, mechanics and geometrics properties.

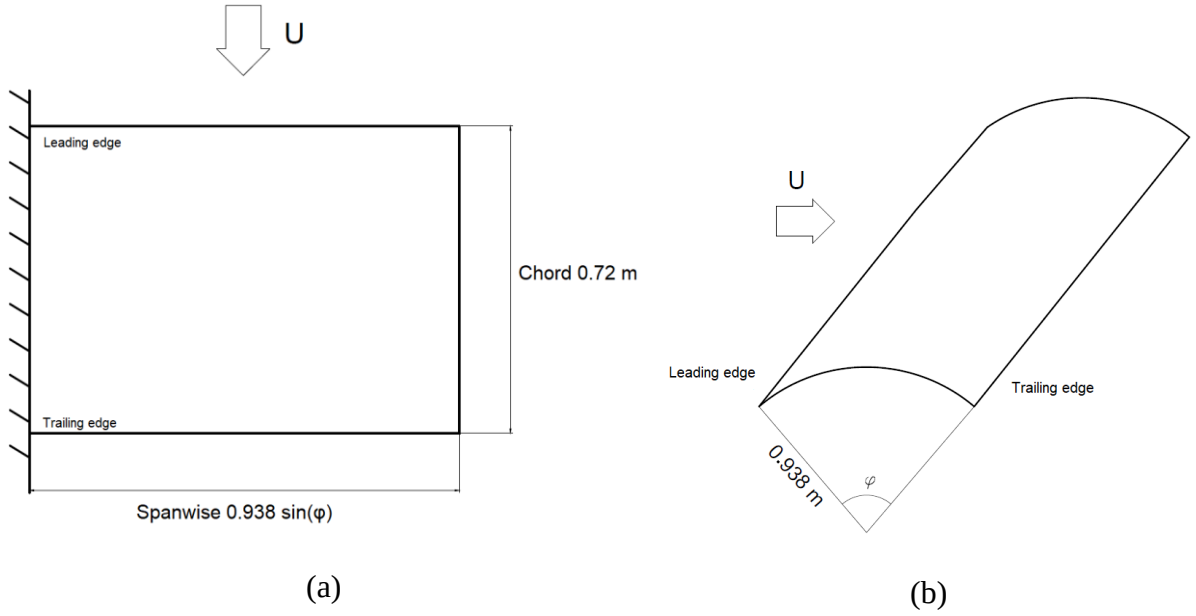

Figure 5. Schematic representation of the curved plate used for the simulations.

Table 2 – Mechanical properties of the material used in the simulation of the curved plate.

MECHANICAL PROPERTIES		
VARIABLES	**VALUES**	**DESCRIPTION**
E	210(GPa)	Young Module
ρ	7800(kg/m³)	Density
υ	0,30	Poisson's Coefficient

Table 3 – Geometrics properties used in the simulation of the curved plate.

GEOMETRICS PROPERTIES	
VARIABLES	**VALUES**
Spanwise	$r\ sin(\varphi)$ (m)
Chord	0,720 (m)
Plate angle (φ)	Variable (º)
Inner radius curvature (r)	0,938 (m)
Thickness (z_i)	r
Thickness (z_o)	$r\ cos(\varphi/180)$

Thus, in this stage it is taken five different angles (10°, 20, 30°, 45° e 70°) and the respective natural frequencies to the two modes of vibration. Furthermore, a mesh of 36 elements is used for both the structural and aerodynamic to calculate de critical flutter speed.

Table 4 – Natural frequencies to the curved plate without viscoelastic material.

ANGLE	**CURVED PLATE WITHOUT VISCOELASTIC MATERIAL**	
	MODE	**FREQUENCY(Hz)**
10°	1	24.3818
	2	28.0603
20°	1	6.1276
	2	9.1379

30°	1	2.7367
	2	5.1417
45°	1	1.2276
	2	2.9712
70°	1	0.5183
	2	1.5017

In the way, the study of the critical flutter speed begins using the code implemented in MATLAB® and considering the Tab. 5 with de aerodynamics properties.

Table 5 – Aerodynamics properties to the flow used in the simulations.

AERODYNAMICS PROPERTIES	
VARIABLES	**VALUES**
Number of panels (chord)	6
Number of panels (spanwise)	6
Mach number	0.25
Density	1.1839 (kg/m³)
Temperature	25°
Reduced frequency	0-3.6
Flutter method	P-K

After the first stage of simulations, some observations are made in relation to the simulated results in the Fig. 6: a) as the angle of the curved plate increases without viscoelastic material, there is a reduction in the critical flutter speed. Qualitatively, this fact can be noted in Fig. 6.a; b) for all previous cases studied, the flutter phenomenon occurs in the second mode of vibration; c) by Fig. 6.b, the flutter frequency reduces as the angle is increased.

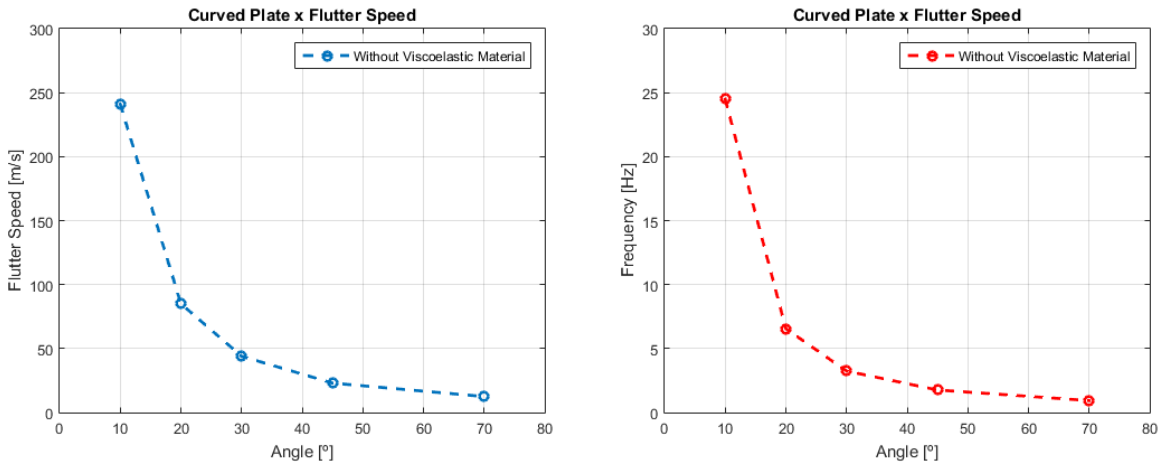

(a) (b)

Figure 6. Comparison of the flutter phenomenon for the curved plate without viscoelastic material being: (a) flutter speed and (b) natural frequencies.

7.2.Curved plate with a thin viscoelastic layer

The proposed case study for the evaluation of the aeroviscoelastic model consists of a curved sandwich plate with a thin intermediate layer with 3M ISD112 viscoelastic material. So, in Tab.6 and 7 are, respectively, the geometric and mechanical properties used in the simulations. It is worth mentioning that the operating temperature will be 25℃ and 36 mesh elements are used for both the structure and the aerodynamic model.

Table 6 – Geometrics properties used in the simulation of the curved sandwich plate with a thin intermediate viscoelastic layer.

GEOMETRICS PROPERTIES			
LAYER	**CHORD(mm)**	**SPANWISE(mm)**	**THICKNESS(mm)**
Base	720	$r\ sin(\varphi)$	1.5
Viscoelastic	720	$r\ sin(\varphi)$	0.0254
Constraining	720	$r\ sin(\varphi)$	0.5

Table 7 – Mechanical properties used in the simulation of the curved sandwich plate with a thin intermediate viscoelastic layer.

MECHANICAL PROPERTIES			
LAYER	**MODULUS OF ELASTICITY(GPa)**	**POISSON'S COEFFICIENT**	**DENSITY (kg/m³)**
Base	210	0,30	7800
Viscoelastic	-	0,49	950
Constraining	210	0,30	7800

In Fig. 7, simulations were performed, for each five angles of the present work, the calculation of the Frequency Response Function (FRF) curves for the curved plate without and with viscoelastic material. The objective of this simulation was to verify the damping of the structures and the comparability of it. Therefore, it can be seen that the viscoelastic material was able to reduce the oscillation amplitudes of the structure as well as increase the natural frequencies. This fact occurs due to the dissipative properties of this type of material, making it an excellent form of passive control. Thus, in the Tab. 8 can be seen the comparison between the natural frequencies of the curved plate for the cases studied.

Table 8 – Comparison of natural frequencies between the curved plate without viscoelastic material and the curved sandwich plate with viscoelastic layer.

ANGLE	**CURVED PLATE WITH VISCOELASTIC MATERIAL**		**CURVED PLATE WITHOUT VISCOELASTIC MATERIAL**	
	MODE	**FREQUENCY(Hz)**	**MODE**	**FREQUENCY(Hz)**
10°	1	43.4807	1	24.3818
	2	53.3692	2	28.0603
20°	1	11.0253	1	6.1276
	2	19.5602	2	9.1379
30°	1	4.9878	1	2.7367
	2	11.6114	2	5.1417
45°	1	2.2955	1	1.2276
	2	6.8945	2	2.9712
70°	1	1.0202	1	0.5183
	2	3.5018	2	1.5017

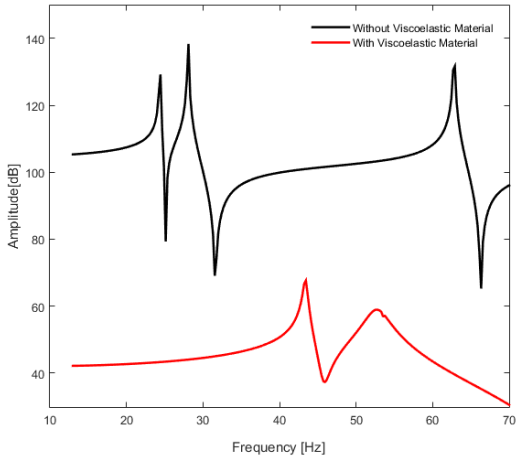
Without Viscoelastic Material
With Viscoelastic Material
Amplitude[dB]
Frequency [Hz]

(a)

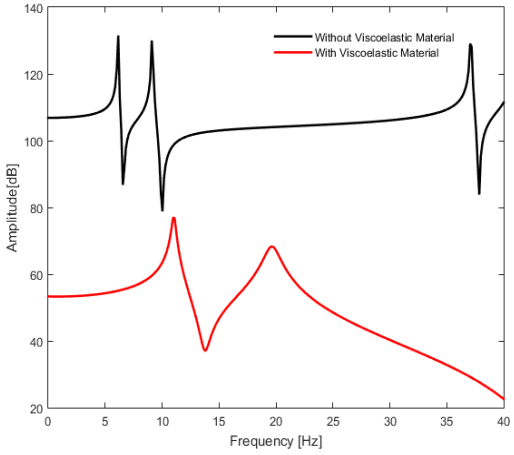
Without Viscoelastic Material
With Viscoelastic Material
Amplitude[dB]
Frequency [Hz]

(b)

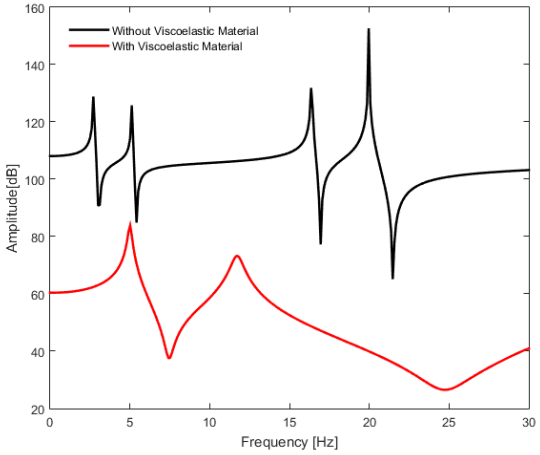
Without Viscoelastic Material
With Viscoelastic Material
Amplitude[dB]
Frequency [Hz]

(c)

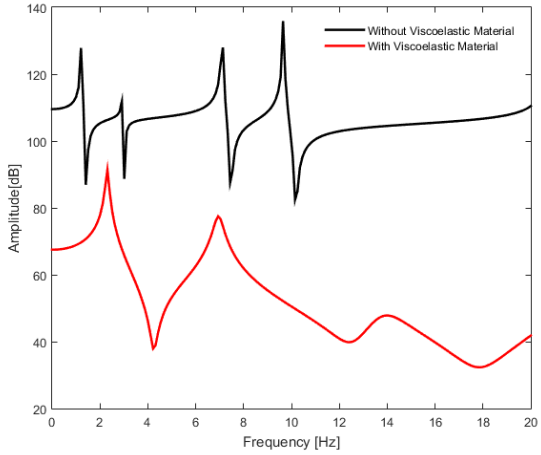
Without Viscoelastic Material
With Viscoelastic Material
Amplitude[dB]
Frequency [Hz]

(d)

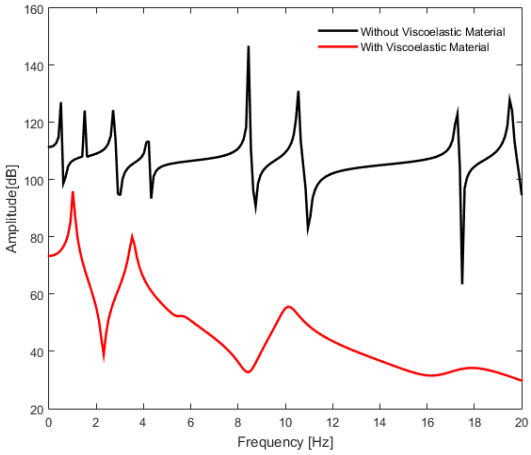
Without Viscoelastic Material
With Viscoelastic Material
Amplitude[dB]
Frequency [Hz]

(e)

Figure 7. Frequency response function (FRF) for the curved plate with and without viscoelastic material where: (a) 10º angle, (b) 20º angle, (c) 30º angle, (d) 45º angle, (e)70° angle.

In this second analysis phase, with the study of the flutter phenomenon in a curved sandwich plate with a thin intermediate layer of the viscoelastic material, facts similar to the previous study were observed in the Fig. 8: a) with the increase of the angulation of the plate, the critical flutter velocity decreased; b) flutter occurs in the second mode for all angles evaluated; c) the flutter frequency decreases as the angle increases.

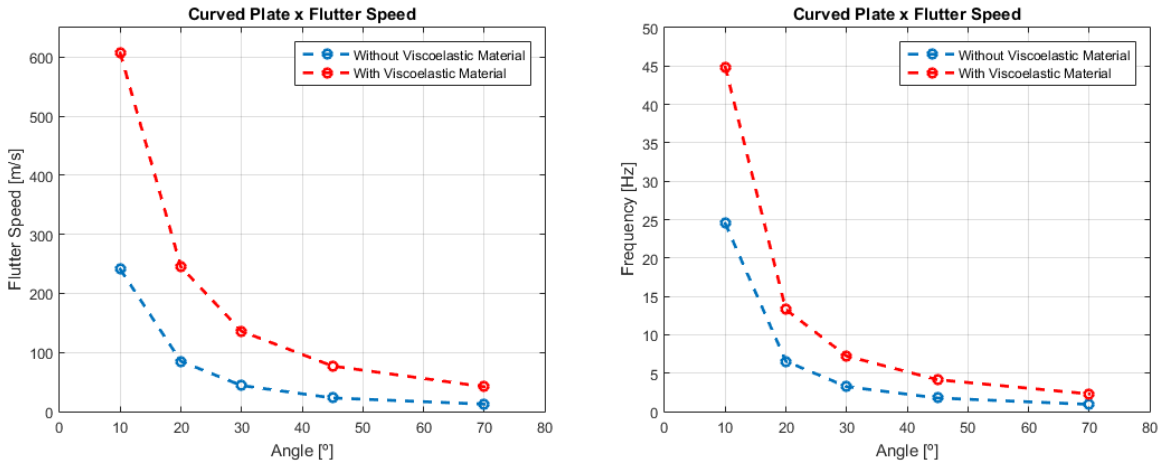

(a) (b)

Figure 8. Comparison of the flutter phenomenon for the curved plate with and without viscoelastic material being: (a) flutter speed and (b) natural frequencies.

So, the viscoelastic materials are characterized by dependence on operating factors such as frequency and temperature. Therefore, these aspects are capable of modifying the stiffness conditions and, consequently, the dissipation of the global structure. Therefore, it is necessary to study these to verify the aeroviscoelastic behavior of the dynamic system. In the first two parts, the operating frequency was explored, keeping the operating temperature set at 25ºC. At this point, the geometric parameters are fixed and a curved sandwich plate with an angle of 30° for various temperatures is analyzed in the Fig.9 .

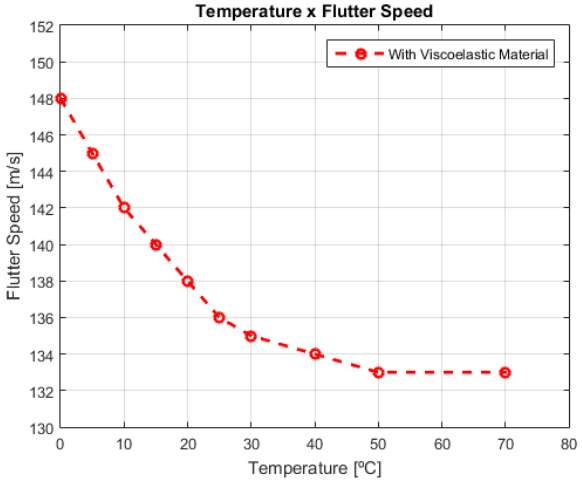

Figure 9. Influence of the operating temperature for the viscoelastic material in relation to the critical flutter speeds for a curved sandwich plate with an angle of 30º.

8.Concluding remarks

In the present work, has been showed a contribution to the recently development of the study about viscoelastic treatment in dynamics systems that have been submitted in the flutter phenomenon, consequently, the passive control of it.

Considering the results of the simulations have been carried out with curve sandwich plate containing viscoelastic damping, it has been proven that the viscoelastic materials have feasibility for use in aeronautical panels with the objective of delaying the occurrence of the flutter phenomenon. In this case, such materials may present an alternative to the application of existing structures for the suppression of flutter phenomenon, because it is a passive control of easy implementation in the structure and provides low cost of maintenance.

Another factor that must be taken into account in the design of aeroviscoelastic systems is the operating temperature, since it usually extreme variations of it during the flight and can influence a direct impact on the performance of the superficial viscoelastic treatment. In general, increasing the operating temperature of the aeroviscoelastic system leads to a decrease the efficiency of it in terms of the attenuation of the critical flutter velocity that could be observed in the Fig. 9.

Therefore, in this article the first part of remark results refers to the associated conservative system which showed the curved plate without viscoelastic material. Then, the second part, has the insertion of the dynamic viscoelastic stiffness that increases the flutter velocity for all angles studied. Therefore, it is believed that this strategy can be advantageously used to the studies about passive control of flutter phenomenon.

9.Acknowledgements

The authors are grateful to the Minas Gerais State Agency FAPEMIG for the financial support to their research activities and the Brazilian Research Council – CNPq for the continued support to their research work. Also, the authors express their acknowledgments to the INCT-EIE, jointly funded by CNPq, CAPES and FAPEMIG.

References

[1] ALBANO, E.; RODDEN, W. P. A doublet-lattice method for calculating lift distributions on oscillating surfaces in subsonic flows. AIAA journal, v. 7, n. 2, pp. 279-285, 1969. https://doi.org/10.2514/3.5086

[2] ALYANAK E. J.; PENDLETON E. Aeroelastic tailoring and active aeroelastic wing impact on a lambda wing configuration. Journal of Aircraft, v. 54, pp. 11-19, 2017. https://doi.org/10.2514/1.C033040

[3] ASHLEY, H. On making things the best-aeronautical uses of optimization. Journal of Aircraft, v. 19, n. 1, pp. 5-28, 1982. https://doi.org/10.2514/3.57350

[4] BAGLEY, R. L.; TORVIK, P. J. A. Fractional calculus – A different approach to the analysis of viscoelastically damped structures. AIAA Journal, v. 21, n. 5, pp. 741-748, 1983. https://doi.org/10.2514/3.8142

[5] BAGLEY, R. L.; TORVIK, P. J. A. Fractional calculus in the transient analysis of viscoelastically damped structures. The American Institute of Aeronautics and Astronautics Journal. v. 23, n. 6, p. 918-925, 1985. https://doi.org/10.2514/3.9007

[6] BAKER, M. L.; RODDEN, W. P. Improving the convergence of the doublet-lattice method through tip corrections. Journal of Aircraft, v. 38, n.4, pp. 772–776. 2001. https://doi.org/10.2514/2.2831

[7] BAVASTRI, C.; FEBBO, M.; GONÇALVES, V.; LOPES, E. Optimum viscoelastic absorbers for cubic nonlinear systems. Journal of Vibration and Control, v. 20, n. 10, pp. 1464–1474. 2013. https://doi.org/10.1177/1077546312473322

[8] BISMARCK-NASR M. N. Kernel function occurring in subsonic unsteady potential flow, AIAA Journal, v. 29, n. 6, pp. 878–879, 1991. https://doi.org/10.2514/3.10673

[9] BLAIR, MAX. A compilation of the mathematics leading to the doublet-lattice method. Airforce Wright Laboratory. Final Report, Ohio 45433-7542, Nov. 1994.

[10] BOTEZ, R. M.; DOIN, A.; BISKRI, D. E.; COTOI, I.; HAMZA, D.; PARVU, P. Method for flutter aero-servoelastic open loop analysis. Canadian Aeronautics and Space Journal, v. 49, n. 4, pp. 179-190. 2003. https://doi.org/10.1115/IMECE2002-33623
[11] BRENDEL, M.; SULAEMAN, E. Improved doublet lattice formulation for calculating aerodynamic loads on lifting surfaces in unsteady subsonic flow. 12th Applied Aerodynamics Conference.1994. https://doi.org/10.2514/6.1994-1890
[12] CUNHA, B. S. C. Controle passivo de vibrações induzidas por vórtices utilizando materiais viscoelásticos. 2016. 104 f. Dissertação de Mestrado - Universidade Federal de Uberlândia, Uberlândia, MG, Brasil. https://doi.org/10.14393/ufu.di.2016.553
[13] CUNHA-FILHO, A. G.; LIMA, A. M. G.; DONADON, M. V.; LEÃO, L. S. Flutter suppression of plates using passive constrained viscoelastic layers. Mechanical Systems and Signal Processing, v. 79, pp. 99-111, 2016. https://doi.org/10.1016/j.ymssp.2016.02.025
[14] GALUCIO, A.C.; DEÜ, J.F.; OHAYON, R. Finite element formulation of viscoelastic sandwich beams using fractional derivative operators. Computational Mechanics, v.33, pp. 282-291, 2004. https://doi.org/10.1007/s00466-003-0529-x
[15] GARRICK, I. E.; REED, W.H. Historical development of aircraft flutter. Journal of Aircraft, v.18, n.11, pp. 897-912, 1981. https://doi.org/10.2514/3.57579
[16] GIESING, J. P. Basic principles and double lattice applications in potential aerodynamics. Computational Methods in Potential Aerodynamics. Springer-Verlag, Computational Mechanics Centre, Southampton, 1987.
[17] HARDER, R. L.; RODDEN, W. P. Kernel function for nonplanar oscillating surfaces in supersonic flow. Journal of Aircraft, v. 8, n. 8, pp. 677–679. 1971. https://doi.org/10.2514/3.44292
[18] HASHEMINEJAD S. M.; MOTAALEGHI M. A., Aeroelastic analysis and active flutter suppression of an electro-rheological sandwich cylindrical panel under yawed supersonic flow. Aerospace Science and Technology, v. 42, pp. 118-127. 2015. https://doi.org/10.1016/j.ast.2015.01.004
[19] HASSIG, H. J. An approximate true damping solution of the flutter equation by determinate iteration. Journal of Aircraft, v. 8, n.11, pp. 885-889, 1971. https://doi.org/10.2514/3.44311
[20] INGRAM C. W.; SZWARC W. J. Passive flutter suppression. Journal of Aircraft, v. 13, n.7, pp. 542-543.1976. https://doi.org/10.2514/3.44544
[21] KALMAN, T. P.; RODDEN, WILLIAM P.; GIESING, J. P. Application of the doublet-lattice method to nonplanar configurations in subsonic flow. Journal of Aircraft, v. 8, n. 6, p. 406-413, 1971. https://doi.org/10.2514/3.59117
[22] KOTIKALPUDI, A.; PFIPER, H.; BALAS, G. J. Unsteady aerodynamics modeling for a flexible unmanned air vehicle. AIAA Atmospheric Flight Mechanics Conference, pp. 2854, 2015. https://doi.org/10.2514/6.2015-2854
[23] LASCHKA, B. The pressure, lift and moment distributions on a harmonically oscillating sweptback wing of low aspect ratio at low subsonic speeds; comparison between theory and measurements. Proc. of International Council of the Aeronautical Sciences, fourth congress, pp. 295-313, Paris, 1967.
[24] LIGHTHILL, M. Oscillanting airfoils at high mach number. Journal of Aeronautical Sciences, v. 20, pp. 402-406. 1953. https://doi.org/10.2514/8.2657
[25] LIMA, A. M. G.; FARIA, A. W.; RADE, D. A. Sensitivity analysis of frequency response functions of composite sandwich plates containing viscoelastic layers. Composite Structures, v. 92, n. 2, pp. 364-376, 2010. https://doi.org/10.1016/j.compstruct.2009.08.017
[26] LIMA, A. M. G.; RADE, D. A.; LÉPORE NETO, F. P. An efficient modeling methodology of structural systems containing viscoelastic dampers based on frequency response function substructuring. Mechanical Systems and Signal Processing, v. 23, n. 4, pp. 1272–1281. 2009. https://doi.org/10.1016/j.ymssp.2008.09.005
[27] MERRETT C. G.; HILTON H. H. Elastic and viscoelastic panel flutter in incompressible, subsonic and compressible flows. Journal of Aeroelasticity and Structural Dynamics, v. 2, n. 1 .2010.
[28] MOON S. H., KIM S. J., Active and passive suppressions of nonlinear panel flutter using finite element method. AIAA journal, v. 39, n.11, pp. 2042-2050. 2001. https://doi.org/10.2514/2.1217
[29] PITT, D. M.; GOODMAN, C. B. Flutter calculations using doublet lattice aerodynamics modified by the full potential equations. 28th AIAA/ASME/ASCE/AHS Structures, Structural Dynamics and Materials Conference. Monterrey, CA. 1987. https://doi.org/10.2514/6.1987-882
[30] RODDEN, W.P.; GIESING, J.P; KALMAN, T.P. New developments and applications of the subsonic doublet-lattice method for nonplanar configurations, AGARD Conference Proceedings, CP-80-71, Part II,No 4, 1971. https://doi.org/10.2514/3.59117
[31] RODDEN, W. P.; GIESING, J. P.; KALMAN, T. P. Refinement of the nonplanar aspects of the subsonic doublet-lattice lifting surface method. Journal of Aircraft, v. 9, n. 1, p. 69-73, 1972. https://doi.org/10.2514/3.44322
[32] RODDEN, W. P.; GIESING, J. P.; KALMAN, T. P. Subsonic unsteady aerodynamics for general configurations. Airforce Wright Flight Dynamics Laboratory. Ohio, Vol. I, Part. I, AFFDL-TR-71-5, Nov, 1971. https://doi.org/10.2514/6.1972-26
[33] RODDEN, W. P., JOHNSON, E. H. MSC/NASTRAN Handbook for Aeroelastic Analysis, Version 68, MacNeal-Schwendler Corp., Los Angeles, CA, 1994.
[34] RODDEN, W. P.; TAYLOR, P. F.; MCINTOSH, S. C. Further refinement of the nonplanar aspects of the subsonic doublet-lattice lifting surface method. In: ICAS PROCEEDINGS. pp. 1786-1799. 1996.
[35] RODDEN, W. P.; TAYLOR, P. F.; MCINTOSH, S. C. Further refinement of the subsonic doublet-lattice method. Journal of Aircraft. v. 35, N. 5, pp. 720-727, 1998. https://doi.org/10.2514/2.2382

[36] STANFORD B. K.; JUTTE C. V.; WU K. C. Aeroelastic benefits of tow steering for composite plates. Composite Structures, v. 118, pp. 416-422. 2014.
https://doi.org/10.1016/j.compstruct.2014.08.007
[37] THEODORSEN, T. General theory of aerodynamic instability and the mechanism of flutter. NACA Technical Report, n. 496, Jan, 1935.
[38] VAN ZYL, L. H. Application of the subsonic doublet lattice method to delta wings. Journal of Aircraft, v. 36, n. 3, pp. 609-610.1999. https://doi.org/10.2514/2.2480
[39] VAN ZYL, L. H. Arbitrary accuracy integration scheme for the subsonic doublet lattice method. Journal of Aircraft, v. 35, n. 6, pp. 975–977. 1998
https://doi.org/10.2514/2.2397
[40] VAN ZYL, L. H. Convergence of the subsonic doublet lattice method. Journal of Aircraft, v.35, n. 6, pp. 977-979. 1998.
https://doi.org/10.2514/2.2398
[41] VAN ZYL, L. H. Robustness of the subsonic doublet lattice method. The Aeronautical Journal , v. 107, n. 1071, pp. 257-262. 2003.
https://doi.org/10.1017/S0001924000013324
[42] VAN ZYL, L. H.; MATHEWS, E. H. Aeroelastic analysis of t-tails using an enhanced doublet lattice method. Journal of Aircraft, v. 48, n. 3, pp. 823–831. 2011.
https://doi.org/10.2514/1.C001000